

Radioactive contamination of $\text{SrI}_2(\text{Eu})$ crystal scintillator

P. Belli^a, R. Bernabei^{a,b,*}, R. Cerulli^c, F.A. Danevich^d, E. Galenin^e,
 A. Gektin^e, A. Incicchitti^{f,g}, V. Isaienko^h, V.V. Kobychiev^d,
 M. Laubenstein^c, S.S. Nagorny^d, R.B. Podviiyanuk^d, S. Tkachenko^e,
 V.I. Tretyak^d

^a*INFN sezione Roma "Tor Vergata", I-00133 Rome, Italy*

^b*Dipartimento di Fisica, Università di Roma "Tor Vergata", I-00133, Rome, Italy*

^c*INFN, Laboratori Nazionali del Gran Sasso, I-67100 Assergi (AQ), Italy*

^d*Institute for Nuclear Research, MSP 03680 Kyiv, Ukraine*

^e*Institute for Scintillation Materials, 61001, Kharkiv, Ukraine*

^f*INFN sezione Roma, I-00185 Rome, Italy*

^g*Dipartimento di Fisica, Università di Roma "La Sapienza", I-00185 Rome, Italy*

^h*National University of Kyiv-Mohyla Academy, 04655 Kyiv, Ukraine*

Abstract

A strontium iodide crystal doped by europium ($\text{SrI}_2(\text{Eu})$) was produced by using the Stockbarger growth technique. The crystal was subjected to a characterization that includes relative photoelectron output and energy resolution for γ quanta. The intrinsic radioactivity of the $\text{SrI}_2(\text{Eu})$ crystal scintillator was tested both by using it as scintillator at sea level and by ultra-low background HPGe γ spectrometry deep underground. The response of the $\text{SrI}_2(\text{Eu})$ detector to α particles (α/β ratio and pulse shape) was estimated by analysing the ^{226}Ra internal trace contamination of the crystal. We have measured: $\alpha/\beta = 0.55$ at $E_\alpha = 7.7$ MeV, and no difference in the time decay of the scintillation pulses induced by α particles and γ quanta. The application of the obtained results in the search for the double electron capture and electron capture with positron emission in ^{84}Sr has been investigated at a level of sensitivity: $T_{1/2} \sim 10^{15} - 10^{16}$ yr. The results of these studies demonstrate the potentiality of this material for a variety of scintillation applications, including low-level counting experiments.

*Corresponding author. E-mail: rita.bernabei@roma2.infn.it

Keywords:

SrI₂(Eu) crystal scintillator, Radioactive contamination, Double beta decay

PACS: 29.40.Mc Scintillation detectors, 23.40.-s β decay; double β decay; electron and muon capture

1. Introduction

The strontium iodide was discovered as scintillator by Hofstadter in 1968 [1]. The interest in this material increased in the last few years because of the high light output ($> 100\,000$ photons/MeV) and of the good energy resolution ($\approx 3\%$ at 662 keV), recently reported in refs. [2, 3, 4]. The main properties of SrI₂(Eu) crystal scintillators are presented in Table 1.

Table 1: Properties of SrI₂(Eu) crystal scintillators

Property	Value	Reference
Density (g/cm ³)	4.5 – 4.6	[2, 4, 5]
Melting point (°C)	515	[2]
Structural type	Orthorhombic	[2]
Index of refraction	1.85	[6]
Wavelength of emission maximum (nm)	429 – 436	[2, 4, 5]
Light yield (photons/MeV)	$(68 - 120) \times 10^3$	[2, 4, 7]
Energy resolution (FWHM, %) for 662 keV γ of ¹³⁷ Cs	2.6 – 3.7	[2, 4, 7, 8, 9]
Scintillation decay time (μ s) under X ray / γ ray excitation at 300 K	0.6 – 2.4	[2, 4, 7, 5]

An important advantage of SrI₂(Eu) in comparison to other high resolution scintillators, like for instance LaCl₃(Ce), LaBr₃(Ce), Lu₂SiO₅(Ce), LuI₃(Ce), is the absence of natural long-living radioactive isotopes (as ¹³⁸La in lanthanum and ¹⁷⁶Lu in lutetium). It makes SrI₂(Eu) scintillators promising in various applications, in particular for low counting experiments as e.g. those searching for double β decay.

The main aim of our study was to test the internal radioactive contamination of a $\text{SrI}_2(\text{Eu})$ crystal scintillator. We have also estimated the response of the detector to α particles by using the data of low background measurements where events of ^{214}Po decays (daughter of ^{226}Ra from the ^{238}U chain) were recorded. As a by-product of the measurements, we have derived limits on double β processes in ^{84}Sr .

2. Scintillator, measurements, results and discussion

2.1. Development of $\text{SrI}_2(\text{Eu})$ crystal scintillators

A single crystal of strontium iodide doped by 1.2% of Eu^1 was grown in a quartz ampoule using the vertical Stockbarger method [10]. Anhydrous strontium iodide activated by europium was obtained by the reaction of the strontium carbonate and europium oxide with the hydroiodic acid as described in [1]. After drying, the obtained hydrate was placed in the quartz ampoule for the crystal growth and slowly heated for five days up to 150°C with permanent vacuum pumping. As a next step the ampoule was welded and placed in the Stockbarger growing set-up, the temperature was increased up to 538°C . The crystal was grown with a speed of 20 mm per day as described in [4]. The crystal boule was cut in a dry box filled by pure nitrogen to obtain a near to cylindrical scintillator 13 mm in diameter and 11 mm length (see Fig. 1, left). The crystal was wrapped with PTFE tape and encapsulated using epoxy glue in an oxygen-free high thermal conductivity (OFHC) copper container with a quartz window, all the materials with low level of radioactive contamination. It is shown in Fig. 1, right; as one can see, the crystal scintillator is neither milky nor cracked. However, the scintillator is not of exact cylindrical shape.

2.2. Energy resolution and relative pulse amplitude

In order to investigate its scintillation properties, the $\text{SrI}_2(\text{Eu})$ crystal scintillator was coupled to a 3" Philips XP2412 photomultiplier (PMT) with a bialkali photocathode using Dow Corning Q2-3067 optical couplant. The detector was irradiated with γ quanta from ^{60}Co , ^{137}Cs , ^{207}Bi , ^{232}Th and

¹We present data on the nominal concentration of Eu in the initial powder used for the crystal growth. The concentration of Eu in the crystal may be lower due to unknown segregation of Eu in SrI_2 . Moreover we cannot exclude some nonuniformity of Eu distribution in the crystal volume and, therefore, presence of concentration gradient of Eu.

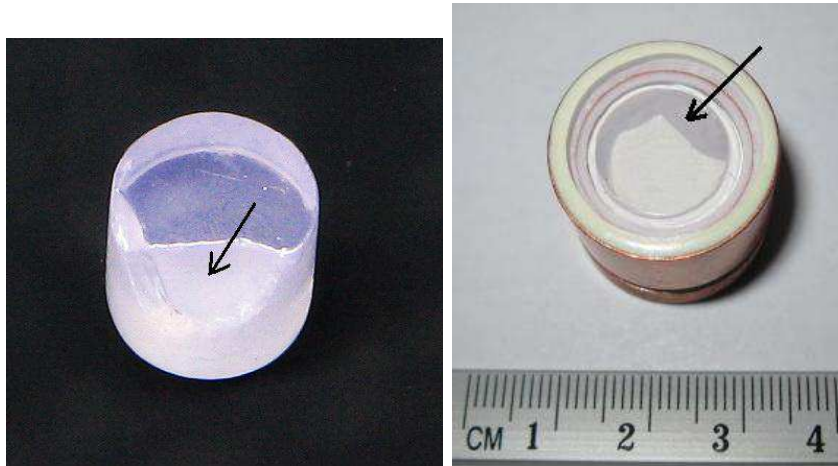


Figure 1: (Color online) Left: $\text{SrI}_2(\text{Eu})$ crystal before encapsulation. Right: Low background $\text{SrI}_2(\text{Eu})$ scintillation detector. Arrows show irregularity of the crystal shape.

^{241}Am γ sources. The measurements were carried out using an ORTEC 572 spectrometric amplifier with $10 \mu\text{s}$ shaping time and a peak sensitive analog-to-digital converter. Fig. 2 shows the pulse amplitude spectra measured by the $\text{SrI}_2(\text{Eu})$ scintillator with ^{60}Co , ^{137}Cs , ^{207}Bi and ^{241}Am γ sources, respectively. The energy resolution FWHM for the 662 keV γ line of ^{137}Cs is 5.8%; it is worse than the best reported results (FWHM = 2.6% – 3.7% at 662 keV) [2, 4, 7, 9]. This fact is probably due to not enough high level of the initial purity of the used powder, to not perfect technology of the crystal production (which is under development now), to a lower amount of the Eu dopant and to a possible concentration gradient of the Eu in the crystal. Besides, some degradation of the energy resolution can be due to the irregular shape of the crystal (a clear effect of the shape of the $\text{SrI}_2(\text{Eu})$ scintillators on the energy resolution is reported in [8]). Moreover, we have used a bialkali PMT, while PMTs with a super-bialkali photocathodes have been applied in the works [2, 4, 7, 8, 9].

The energy resolution of the $\text{SrI}_2(\text{Eu})$ crystal scintillator measured in the (60 – 2615) keV energy range is presented in Fig. 3. According to [11, 12] the data were fitted (by the chi-square method; $\chi^2/n.d.f. = 9.5/5 = 1.9$, where n.d.f. is number of degrees of freedom) by the function $\text{FWHM}(\%) = \sqrt{a + b/E_\gamma}$ (where E_γ is the energy of the γ quanta in keV) with parameters

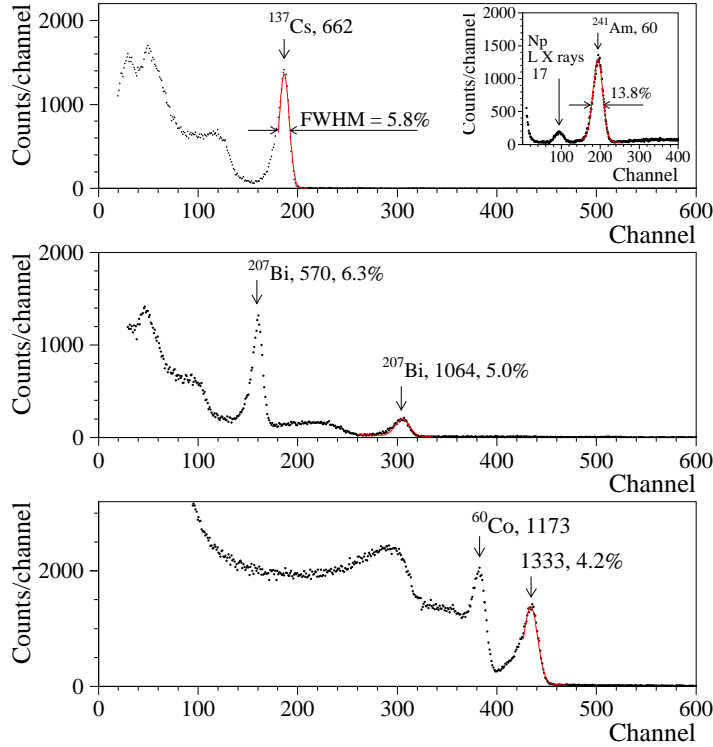


Figure 2: (Color online) Energy spectra of ^{137}Cs , ^{241}Am (inset), ^{207}Bi , and ^{60}Co γ rays measured with the $\text{SrI}_2(\text{Eu})$ scintillation crystal. Energies of the γ lines are in keV.

$a = (10 \pm 2)$ and $b = (14200 \pm 1500)$ keV. The relative pulse amplitude of the $\text{SrI}_2(\text{Eu})$ detector was found to be 87% of a commercial $\text{NaI}(\text{Tl})$ scintillator ($\varnothing 40 \text{ mm} \times 40 \text{ mm}$) (see Fig. 4).

It is rather difficult to derive a photon yield value from the measurements; indeed, one should know both the light collection and the PMT quantum efficiency for the scintillation detectors. It should be stressed that the calculations of the light collection in scintillation detectors is a rather complicated problem. In addition, we do not know an emission spectrum of our sample, while in literature there are different data on this [2, 4, 5]. Nevertheless, taking into account: i) the comparable emission spectra of $\text{SrI}_2(\text{Eu})$ and of $\text{NaI}(\text{Tl})$ (maximum at 429 – 436 nm and at 415 nm, respectively); ii) the relatively flat behaviour of the PMT spectral sensitivity in the region (400 – 440) nm; iii) the typical light yield of $\text{NaI}(\text{Tl})$ in literature: $\approx 40 \times 10^3$

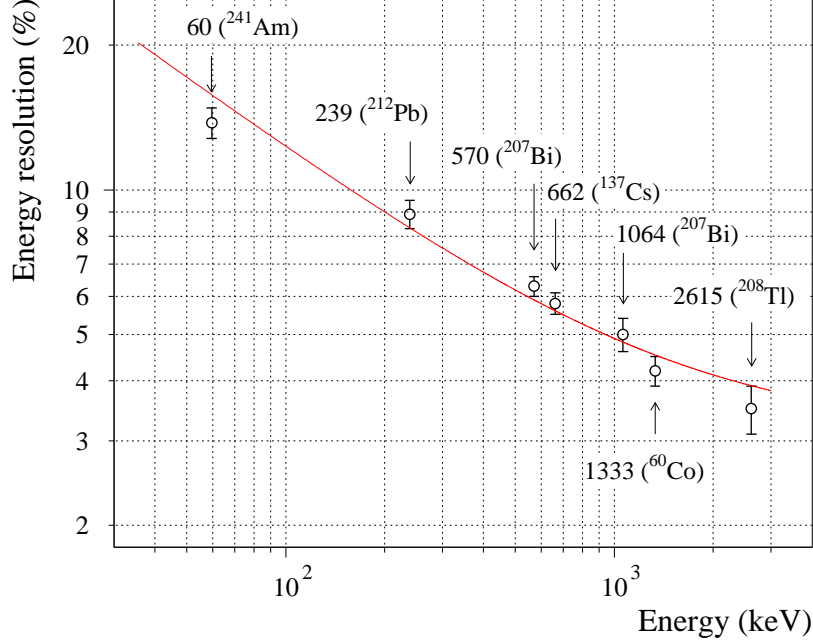


Figure 3: Energy resolution (FWHM) versus γ energy, measured by the $\text{SrI}_2(\text{Eu})$ crystal scintillator.

photons/MeV, we can conclude that the light yield of the sample under study is still far from the best reported $(68 - 120) \times 10^3$ photons/MeV [2, 4, 7].

2.3. Low background measurements in scintillation mode at sea level

The radioactive contamination of the crystal was measured in the low background set-up installed at sea-level in the Institute for Nuclear Research (INR, Kyiv, Ukraine). In the set-up, a $\text{SrI}_2(\text{Eu})$ crystal scintillator was optically connected to a 3" photomultiplier tube Philips XP2412 through a high purity polystyrene light-guide ($\varnothing 66 \times 120$ mm). The optical contact between the scintillation crystal, the light-guide and the PMT was provided by Dow Corning Q2-3067 optical couplant. The light-guide was wrapped with aluminised Mylar. The detector was surrounded by a passive shield made of OFHC copper (5-12 cm thick), and lead (5 cm thick). After the first run of measurements over 52 h, an anti-muon veto counter was installed above the set-up. The counter consists of polystyrene based plastic scintillator $50 \times 50 \times 8$ cm viewed by a low background PMT FEU-125 (Ekran

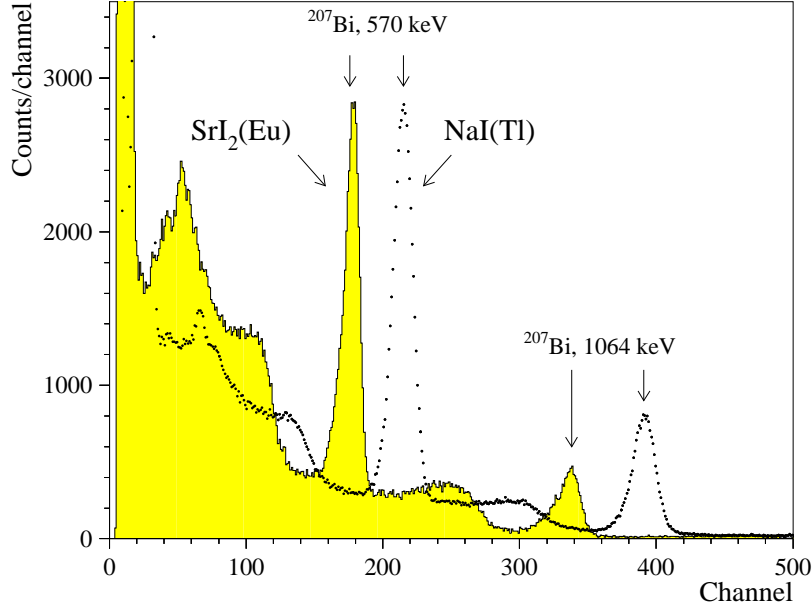


Figure 4: Energy spectra of ^{207}Bi γ rays measured by the $\text{SrI}_2(\text{Eu})$ and by a commercial $\text{NaI}(\text{Tl})$ scintillation detectors in the low background set up at sea level.

Optical Systems, Russia) with a diameter of the photocathode equal to 15 cm. The anti-muon shield suppressed the background caused by cosmic rays by a factor ≈ 3 (at the energy ≈ 4 MeV).

An event-by-event data acquisition system has recorded the pulse shape of the $\text{SrI}_2(\text{Eu})$ scintillator over a time window of $100 \mu\text{s}$ (by using a 20 MS/s 12 bit transient digitizer [13]), the arrival time of the signals (with an accuracy of $0.3 \mu\text{s}$), and the signals amplitude by a peak sensitive analog-to-digital converter.

The energy scale and the energy resolution of the detector were determined in calibration runs by ^{60}Co , ^{137}Cs and ^{207}Bi γ ray sources. The energy resolution becomes slightly worse due to the light-guide used in the low background set-up. It can be fitted by a function: $\text{FWHM}(\%) = \sqrt{a + b/E_\gamma}$ with parameters $a = (7.4 \pm 4.2)$ and $b = (28100 \pm 8000)$ keV, where E_γ is the energy of the γ quanta in keV.

A search for the fast chain ^{214}Bi ($Q_\beta = 3272$ keV, $T_{1/2} = 19.9$ m) \rightarrow ^{214}Po ($Q_\alpha = 7833$ keV, $T_{1/2} = 164 \mu\text{s}$) \rightarrow ^{210}Pb of the ^{238}U family was

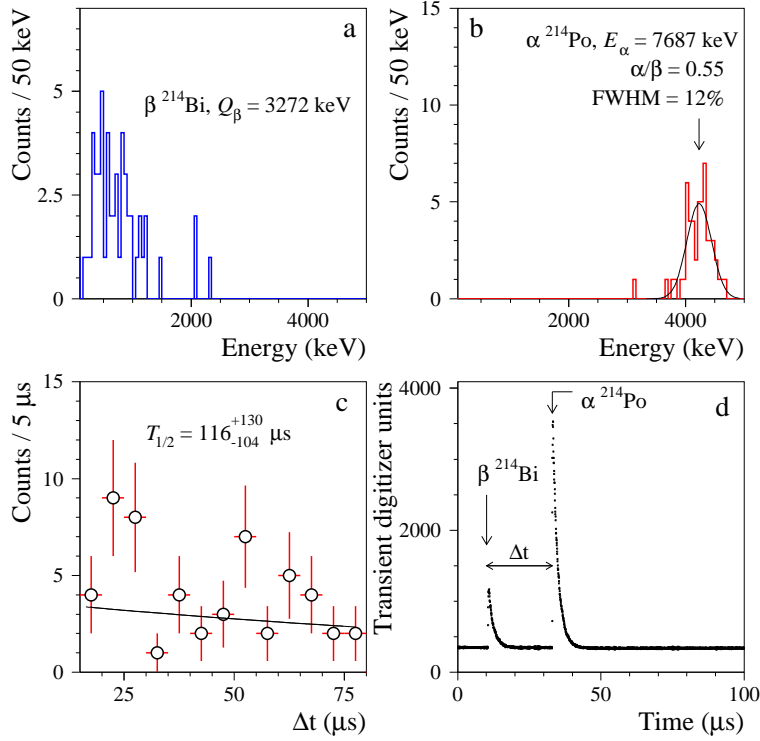


Figure 5: (Color online) The energy (a) and (b), and time (c) distributions for the fast sequence of β (^{214}Bi , $Q_\beta = 3272$ keV) and α (^{214}Po , $E_\alpha = 7687$ keV, $T_{1/2} = 164.3(20)$ μs [16]) decays by the analysis of double pulses in the background data accumulated over 101.52 h. (d) Example of such an event in the $\text{SrI}_2(\text{Eu})$ scintillator.

performed by analysing the double pulses (see the technique of the double pulse analysis e.g. in [14, 15]); the result of the analysis is presented in Fig. 5. The obtained energy spectra of the first and second events, as well as the time distribution between the signals can be explained by the fast $^{214}\text{Bi} - ^{214}\text{Po}$ decay sequence. Taking into account the detection efficiency in the time window (15 – 77) μs (it contains 21.6% of ^{214}Po decays), the mass of the crystal 6.6 g, the measuring time 101.52 h and the number of selected events (52), one can estimate the activity of ^{226}Ra in the $\text{SrI}_2(\text{Eu})$ crystal as 100(14) mBq/kg.

By using the result of the double pulses analysis, we have estimated the response of the $\text{SrI}_2(\text{Eu})$ crystal scintillator to α particles. The quenching of

the scintillation light yield can be expressed through the so called α/β ratio, which is the ratio of the position of an α peak in the energy scale measured with γ quanta to the energy of the α particles. Considering the spectrum presented in Fig. 5(b) as given by α particles of ^{214}Po with energy 7687 keV, we can estimate the α/β ratio as 0.55. A similar quenching was observed in ref. [17] for NaI(Tl) ($\alpha/\beta = 0.66$) and CsI(Tl) ($\alpha/\beta = 0.67$) crystal scintillators with the α particles of a ^{241}Am source with energy 5.48 MeV; in ref. [18] similar values have been measured in ultra low background NaI(Tl) for α trace contaminants internal to the crystals. It should be stressed that the energy resolution for the α peak of ^{214}Po ($\text{FWHM}_\alpha = 12\%$) is worse than that expected at the energy ≈ 4.2 MeV according to the calibration with γ sources ($\text{FWHM}_\gamma \approx 3\%$). A similar effect was observed in crystal scintillators with anisotropic crystal structure, as for instance in CdWO_4 [14] and ZnWO_4 [19].

A search for internal contamination of the crystal by ^{228}Th (daughter of ^{232}Th) was realized with the help of the time-amplitude analysis². To determine the activity of ^{228}Th , the following sequence of α decays was selected: ^{220}Rn ($Q_\alpha = 6405$ keV, $T_{1/2} = 55.6$ s) \rightarrow ^{216}Po ($Q_\alpha = 6907$ MeV, $T_{1/2} = 0.145$ s) \rightarrow ^{212}Pb . Assuming that the α/β ratio for the α particles of (6.3 – 7.7) MeV is in the range of 0.5 – 0.6, the energy interval for both α particles was chosen as (2.8 – 4.5) MeV. The result of the selection is presented in Fig. 6.

Despite the low statistics (only 12 pairs were found), the positions of the selected events and the distribution of the time intervals between the events do not contradict the expectations for the α particles of the chain. Taking into account the efficiency in the time window (0.01 – 0.5) s to select $^{216}\text{Po} \rightarrow ^{212}\text{Pb}$ events (86.2%), the activity of ^{228}Th in the crystal can be calculated as 6(2) mBq/kg.

The energy spectrum measured with the $\text{SrI}_2(\text{Eu})$ scintillator over 101.52 h is presented in Fig. 7. There is a peak in the spectrum at the energy of (665 ± 5) keV, which can be explained by contaminations of the $\text{SrI}_2(\text{Eu})$ detector or/and of the set-up by ^{137}Cs (probably as a result of pollution after the Chernobyl accident). Taking into account that our set-up is installed at sea level, a significant part of the background above 2.6 MeV (the edge of the γ quanta energy from the natural radioactivity) can be attributed to cosmic rays.

²The method of the time-amplitude analysis is described in detail in [20, 21].

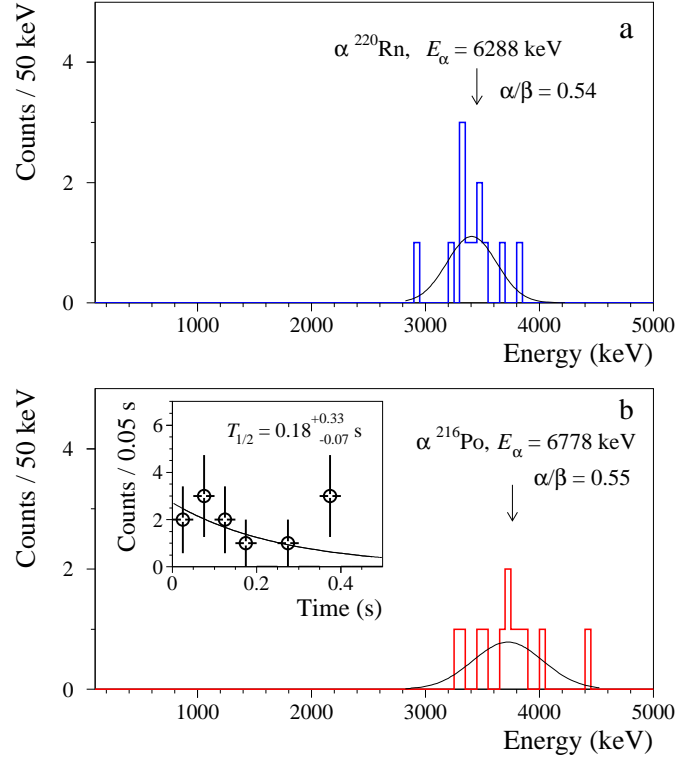


Figure 6: (Color online) Energy spectra of the first (a) and second (b) events selected by the time-amplitude analysis (see text) from the background data accumulated over 101.52 h with the $\text{SrI}_2(\text{Eu})$ detector. In the inset the time distribution between the first and second events together with an exponential fit are presented. The positions of the selected events (solid lines represents fit of the data by Gaussian functions) and the obtained half-life of ^{216}Po ($0.18^{+0.33}_{-0.07} \text{ s}$, the table value is $0.145(2) \text{ s}$ [16]) do not contradict the assumption that these events are caused by the sequence of α decays $^{220}\text{Rn} \rightarrow ^{216}\text{Po} \rightarrow ^{212}\text{Pb}$.

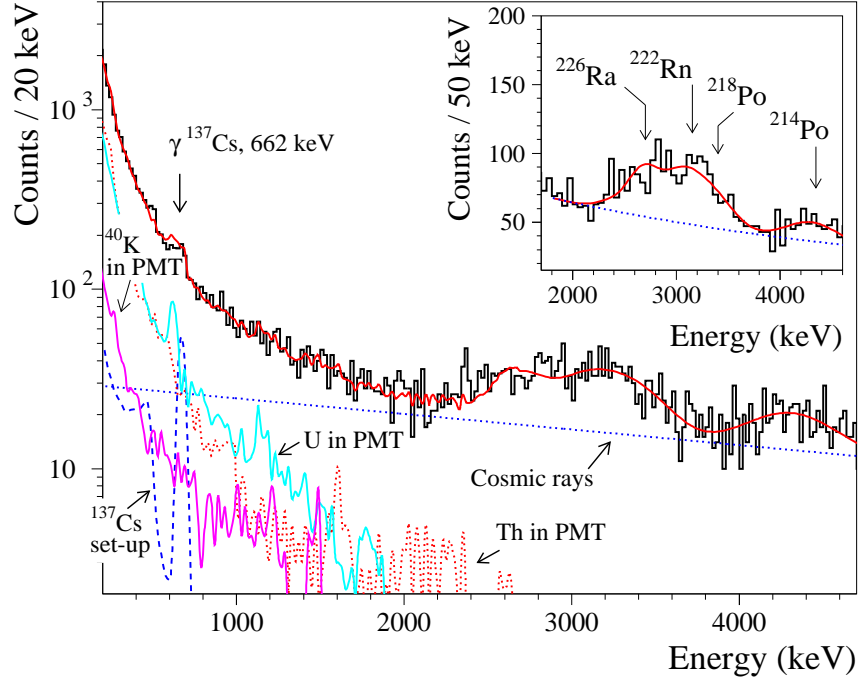


Figure 7: (Color online) Energy spectrum of the $\text{SrI}_2(\text{Eu})$ scintillator measured over 101.52 hours together with the model of the background. The main components of the external background (^{137}Cs on details of the set-up, ^{40}K , U and Th in PMT) and of the cosmic rays are shown (see text for details). (Inset) Increase of the counting rate in the energy region (2.5 – 4.3) MeV is due to α activity of trace U/Th contamination (mainly ^{226}Ra with its daughters) of the crystal scintillator.

Peculiarities in the spectrum in the energy region (2.5 – 4.5) MeV can be explained by the decays of α active U/Th daughters present in the crystal as trace contamination. To estimate the activity of the α active nuclides from the U/Th families in the crystal, the energy spectrum was fitted in the energy interval (1.8 – 4.7) MeV by using fourteen Gaussian functions to describe α peaks of ^{232}Th , ^{228}Th (and daughters: ^{224}Ra , ^{220}Rn , ^{216}Po , ^{212}Bi), ^{238}U (and daughters: ^{234}U , ^{230}Th), ^{226}Ra with daughters (^{222}Rn , ^{218}Po , ^{214}Po , ^{210}Po)³ plus an exponential function to describe background⁴. A fit of the

³We assume a broken equilibrium of the U/Th chains in the scintillator.

⁴At sea level the energy spectrum of cosmic ray induced background in different nuclear detectors, including scintillating, has a monotonic character, which can be approximated in

spectrum is shown in the Inset of Fig. 7. The main contribution to the α activity in the scintillator gives an activity (91 ± 8) mBq/kg for the ^{226}Ra and daughters (^{222}Rn , ^{218}Po and ^{214}Po). This estimate is in agreement with the result of the double pulse analysis (100 ± 14 ; mBq/kg, see above) and with the measurements performed deep underground with ultra-low background HPGe γ ray spectrometry (Section 2.5). Because of the low statistics and of the relatively poor energy resolution for α particles, we conservatively give limits on activities of ^{232}Th , ^{238}U and ^{210}Po in the $\text{SrI}_2(\text{Eu})$ scintillator. The data obtained from the fit are presented in Table 2.

To estimate the contamination of the scintillator by ^{40}K , ^{60}Co , ^{90}Sr – ^{90}Y , ^{137}Cs , ^{138}La , ^{152}Eu , ^{154}Eu , ^{176}Lu , ^{210}Pb – ^{210}Bi , their decays in the $\text{SrI}_2(\text{Eu})$ detector were simulated with the GEANT4 package [26] and the event generator DECAY0 [27]. The radioactive contamination of the set-up, in particular, the radioactivity of the PMT can contribute to the background, too. Therefore we have also simulated the contribution from the contamination of the PMT by ^{232}Th , ^{238}U (with their daughters) and ^{40}K . An exponential function was adopted to describe the contribution of the cosmic rays in the sea level installation where these measurements were carried out.

Apart from the peak of ^{137}Cs and the α peaks in the energy region (2.5 – 4.3) MeV, there are no other peculiarities in the spectrum which could be ascribed to internal trace radioactivity. However, even in the case of ^{137}Cs we cannot surely distinguish the contribution of internal and external contamination. Therefore, only limits on contaminations of the crystal by the possible radionuclides were set on the basis of the experimental data. With this aim the spectrum was fitted in the energy interval (0.2 – 4.65) MeV by the model composed by the background components (^{40}K , U and Th in PMT, pollution of the set-up surface by ^{137}Cs , the α peaks of ^{226}Ra with daughters, and cosmic rays) plus a distribution of possible internal radioactive contamination to be estimated. The result of the fit is presented in Fig. 7 together with the main components of the background.

The summary on activities (or limits) obtained by the analysis of the experimental data accumulated at the sea level low background scintillation set-up is presented in Table 2.

Despite the sea level location and the modest shield of the scintillation set-up, the measurements allowed the detection of the internal contamination

reasonable narrow energy regions (a few MeV) by an exponential function [22, 23, 24, 25].

of the scintillator by ^{226}Ra and ^{228}Th ; besides, we have estimated limits on activities of ^{238}U , ^{232}Th , ^{210}Pb , ^{210}Po , ^{90}Sr . It should be stressed that these radionuclides are rather hard to analyse with the help of low background HPGe γ spectrometry due to the absence of noticeable γ rays. Moreover, the measurements allowed us to estimate the α/β ratio and to measure the pulse shape for α particles (see the next Section) by recording the pulse profiles of ^{214}Po α events inside the scintillator.

2.4. Pulse shape of scintillation for γ quanta (β particles) and α particles from the sea level measurements

The pulse profiles of 41 α events of ^{214}Po were selected with the help of the double pulse analysis from the data of the low background measurements (see Section 2.3 and Fig. 5). The sum of the pulses is presented in Fig. 8 where also the sum of approximately two thousands of background γ (β) events with energies ≈ 1.5 MeV is drawn.

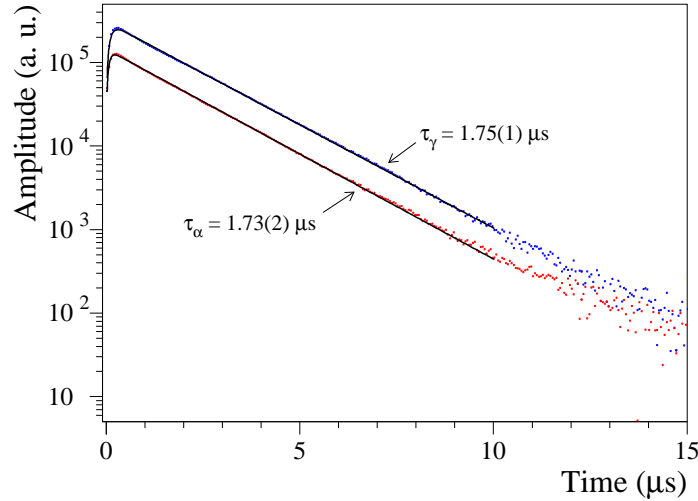


Figure 8: (Color online) Scintillation pulse profiles in the $\text{SrI}_2(\text{Eu})$ crystal measured for γ and α excitation. Fitting functions for γ and α pulses are shown by solid lines.

The distributions were fitted in the time interval $(0 - 10)$ μs by the following function:

$$f(t) = A(e^{-t/\tau} - e^{-t/\tau_0})/(\tau - \tau_0), \quad t > 0,$$

where A is the intensity (in arbitrary units), and τ is the decay constant of the light emission; τ_0 is the integration constant of the electronics ($\approx 0.08 \mu\text{s}$). The fit gives the scintillation decay times in the $\text{SrI}_2(\text{Eu})$ crystal scintillator: $\tau_\gamma = (1.75 \pm 0.01) \mu\text{s}$ and $\tau_\alpha = (1.73 \pm 0.02) \mu\text{s}$ for γ quanta (β particles) and α particles, respectively. Therefore we have not observed any clear indication on differences in the kinetics of the scintillation decay in the $\text{SrI}_2(\text{Eu})$ crystal scintillator under γ quanta (β particles) and α particles irradiation.

2.5. Measurements with ultra-low background HPGe γ ray spectrometry deep underground

The $\text{SrI}_2(\text{Eu})$ crystal scintillator was measured for 706 h with the ultra-low background HPGe γ ray spectrometer GeCris. The detector has a volume of 468 cm^3 and a 120% efficiency relatively to a 3 in. \times 3 in. $\text{NaI}(\text{Tl})$. This detector has a rather thin Cu window of 1 mm thickness. The passive shield of the detector consists of 15 cm of OFHC copper and 20 cm of low radioactive lead. The whole set-up is sealed in an air-tight plexiglass box continuously flushed with high purity nitrogen gas to avoid the presence of residual environmental radon. The facility is located deep underground in the Gran Sasso National Laboratories of the I.N.F.N. (average overburden of 3600 m water equivalent) [28, 29]. The background data were accumulated over 1046 h (see Fig. 9).

In order to determine the radioactive contamination of the sample, the detection efficiencies were calculated using a Monte Carlo simulation based on the GEANT4 software package [26]. The peaks in the measured spectra are due to the naturally occurring radionuclides of the uranium and thorium chains, ^{40}K and ^{137}Cs . We have detected contaminations by ^{137}Cs and ^{226}Ra (the γ lines of ^{137}Cs , ^{214}Bi and ^{214}Pb were observed) in the crystal scintillator at the level of 53(11) mBq/kg and 120(50) mBq/kg, respectively, while limits were obtained for other potential contaminations. The measured activities and the limits are presented in Table 2.

In addition, we have observed the 1157 keV peak of ^{44}Sc in the data accumulated with the $\text{SrI}_2(\text{Eu})$ crystal (at a rate of $6.1(9) \times 10^{-2}$ counts/h). However, this peak was due to a contamination of the used HPGe detector (not of the crystal scintillator sample) by ^{44}Ti .

The radioactive purity of the $\text{SrI}_2(\text{Eu})$ scintillator is still far from that of $\text{NaI}(\text{Tl})$ and $\text{CsI}(\text{Tl})$ scintillators (especially those developed with high radiopurity for dark matter search [18, 30]). At the same time it is much better than the typical purity of $\text{LaCl}_3(\text{Ce})$, $\text{LaBr}_3(\text{Ce})$, $\text{Lu}_2\text{SiO}_5(\text{Ce})$ and $\text{LuI}_3(\text{Ce})$

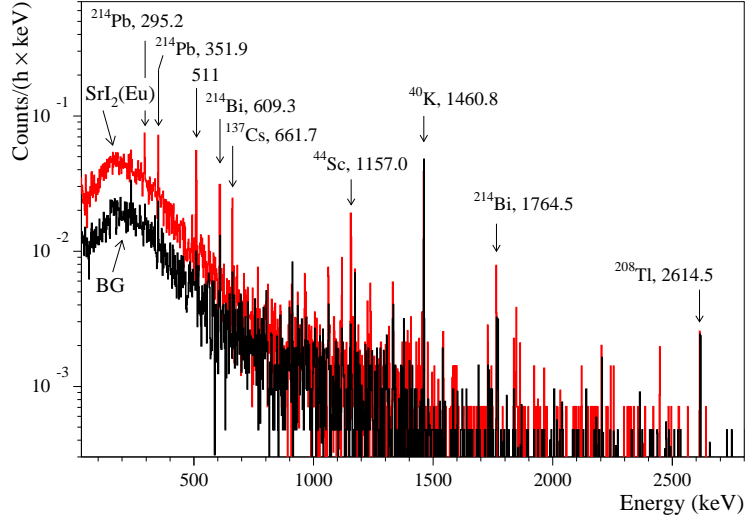


Figure 9: (Color online) Energy spectra accumulated with the $\text{SrI}_2(\text{Eu})$ sample over 706 h, and without sample over 1046 h (BG) by ultra-low background HPGe γ spectrometer deep underground. The energies of the γ lines are in keV. The background was accumulated before the contamination of the HPGe set-up by ^{44}Ti .

crystal scintillators (see Table 3, where the radioactive contamination of the $\text{SrI}_2(\text{Eu})$ crystal is compared with that of $\text{NaI}(\text{Tl})$, $\text{CsI}(\text{Tl})$ and scintillators containing La or Lu).

3. Search for 2β decay of ^{84}Sr

The data of the low background measurements with the HPGe detector can be used to search for double β processes in ^{84}Sr accompanied by the emission of γ quanta. The decay scheme of ^{84}Sr is presented in Fig. 10. The energy of double β decay of ^{84}Sr is comparatively high: $Q_{2\beta} = 1787(4)$ keV [33], however the isotopic abundance is rather low: $\delta = 0.56(1)\%$ [31].

We do not observe any peaks in the spectrum accumulated with the sample of the $\text{SrI}_2(\text{Eu})$ scintillator which could indicate double β activity of ^{84}Sr . Therefore, only lower half-life limits ($\lim T_{1/2}$) can be set according to the formula: $\lim T_{1/2} = N \cdot \eta \cdot t \cdot \ln 2 / \lim S$, where N is the number of ^{84}Sr nuclei in the sample, η is the detection efficiency, t is the measuring time, and $\lim S$ is the number of events of the effect searched for which can be excluded at given confidence level (C.L.; all the limits obtained in the present study

Table 2: Radioactive contamination of the SrI₂(Eu) scintillator. The upper limits are given at 90% C.L., and the uncertainties of the measured activities at 68% C.L.

Chain	Nuclide (Sub-chain)	Activity (mBq/kg)	
		Measured in scintillation mode	Measured by HPGe
	⁴⁰ K	≤ 200	≤ 255
	⁶⁰ Co	≤ 540	≤ 16
	⁹⁰ Sr– ⁹⁰ Y	≤ 90	
	¹³⁷ Cs	≤ 140	53 ± 11
	¹³⁸ La	≤ 1100	≤ 20
	¹⁵² Eu	≤ 840	≤ 108
	¹⁵⁴ Eu	≤ 910	≤ 67
	¹⁷⁶ Lu	≤ 970	≤ 143
²³² Th	²³² Th	≤ 3	
	²²⁸ Ac		≤ 68
	²²⁸ Th	6 ± 2	≤ 52
²³⁸ U	²³⁸ U	≤ 40	
	²²⁶ Ra	100 ± 14	120 ± 50
	²¹⁰ Pb– ²¹⁰ Bi	≤ 180	
	²¹⁰ Po	≤ 60	

are given at 90% C.L.). The efficiencies of the detector for the double β processes in ⁸⁴Sr were calculated with the GEANT4 code [26] and DECAY0 event generator [27].

One positron can be emitted in the $\varepsilon\beta^+$ decay of ⁸⁴Sr with energy up to (765 ± 4) keV. The annihilation of the positron will give rise to two 511 keV γ 's leading to an extra rate in the annihilation peak. The part of the spectrum in the energy interval (450 – 550) keV is shown in Fig. 11.

There are peculiarities in both the spectra accumulated with the SrI₂(Eu) sample [(111 ± 14) counts at (510.9 ± 0.2) keV] and in the background [(12 ± 5) counts at (510.8 ± 0.3) keV], which can be ascribed to annihilation peaks. The main contribution to the 511 keV peak [(108 ± 22) counts] is coming from decays of ⁴⁴Sc (daughter of ⁴⁴Ti) present in the HPGe detector as contamination (see Section 3.4), (8 ± 3) counts corresponds to the background of the detector before the contamination. The difference in the areas of the

Table 3: Radioactive contaminations of $\text{SrI}_2(\text{Eu})$ crystal scintillator. Data for $\text{NaI}(\text{Tl})$, $\text{CsI}(\text{Tl})$, LaCl_3 , $\text{LaBr}_3(\text{Ce})$, Lu_2SiO_5 , $\text{LuI}_3(\text{Ce})$ are given for comparison. Activities of $\text{LaBr}_3(\text{Ce})$, $\text{Lu}_2\text{SiO}_5(\text{Ce})$ and $\text{LuI}_3(\text{Ce})$ are calculated values based on the ^{138}La and ^{176}Lu half-lives [16], on the abundances of the isotopes [31] and on the chemical formula of the compounds.

Scintillator	Activity (mBq/kg)				
	^{40}K	^{138}La	^{176}Lu	^{226}Ra	^{228}Th
$\text{SrI}_2(\text{Eu})^a$	≤ 255	≤ 20	≤ 143	120	≤ 11
$\text{NaI}(\text{Tl})$ [18]	< 0.6			~ 0.02	~ 0.009
$\text{CsI}(\text{Tl})$ [30]				0.009	0.002
$\text{LaCl}_3(\text{Ce})$ [32]		4.1×10^5		≤ 35	≤ 0.36
$\text{LaBr}_3(\text{Ce})$		3.0×10^5			
$\text{Lu}_2\text{SiO}_5(\text{Ce})$			3.9×10^7		
$\text{LuI}_3(\text{Ce})$			1.6×10^7		

^a This work

annihilation peak: (-5 ± 26) counts, which can be attributed to electron capture with positron emission in ^{84}Sr , gives no indication on the effect. In accordance with the Feldman-Cousins procedure [34] (here and hereafter we use this approach to estimate the values of $\lim S$ for all the processes searched for) we should take $\lim S = 38$ counts which can be excluded at 90% C.L. Taking into account the number of ^{84}Sr nuclei in the sample (6.5×10^{19}) and the detection efficiency ($\eta = 7.2\%$), we have calculated the following limit on the half-life of ^{84}Sr relatively to $\varepsilon\beta^+$ decay:

$$T_{1/2}^{(2\nu+0\nu)\varepsilon\beta^+} (\text{g.s.} \rightarrow \text{g.s.}) \geq 6.9 \times 10^{15} \text{ yr.}$$

We cannot study the $2\nu 2K$ capture in ^{84}Sr to the ground state of ^{84}Kr because the energies of the expected X rays after the decay are too low in energy (the binding energy of electrons at K shell of krypton atom is only 14.3 keV [16] while the energy threshold of the HPGe detector is ≈ 20 keV).

In the neutrinoless double electron capture to the ground state of the daughter nucleus, in addition to the X rays, some other particle(s) must be emitted to take away the rest of the energy. Usually one bremsstrahlung γ quantum is assumed. The energy of the γ quantum is expected to be equal to $E_\gamma = Q_{2\beta} - E_{b1} - E_{b2}$, where E_{b1} and E_{b2} are the binding energies of the

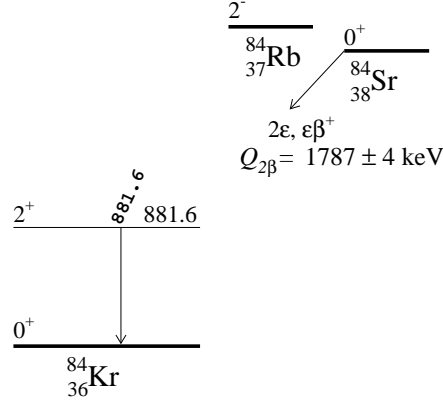


Figure 10: Expected decay scheme of ^{84}Sr [16]. The energies of the excited levels and of the emitted γ quanta are in keV.

first and of the second captured electrons on the atomic shell. The binding energies on the K , L_1 , L_2 and L_3 shells in Kr are equal to $E_K = 14.3$ keV, $E_{L_1} = 1.9$ keV, $E_{L_2} \approx E_{L_3} = 1.7$ keV, respectively [16]. Therefore, the expected energies of the γ quanta for the $0\nu 2\epsilon$ capture in ^{84}Sr to the ground state of ^{84}Kr are in the intervals: i) $E_\gamma = (1754 - 1762)$ keV for the $0\nu 2K$; ii) $E_\gamma = (1767 - 1775)$ keV for the $0\nu KL$; iii) $E_\gamma = (1779 - 1788)$ keV for the $0\nu 2L$ process.

No events are detected (see Fig. 12, a) in the energy intervals (1754 – 1762) and (1779 – 1788) keV, where the g.s. \rightarrow g.s. $0\nu 2K$ and $0\nu 2L$ decay of ^{84}Sr is expected.

According to [34] we should take 2.4 events as $\lim S$. Therefore, taking into account the detection efficiencies of the effects (4.0% and 3.9%, respectively), we can set the following limits on the processes:

$$\begin{aligned}
 T_{1/2}^{0\nu 2K}(\text{g.s.} \rightarrow \text{g.s.}) &\geq 6.0 \times 10^{16} \text{ yr}, \\
 T_{1/2}^{0\nu 2L}(\text{g.s.} \rightarrow \text{g.s.}) &\geq 5.9 \times 10^{16} \text{ yr}.
 \end{aligned}$$

There are 3 events at energy ≈ 1770 keV (due to ^{207}Bi in the background) where the $0\nu KL$ decay of ^{84}Sr is expected. Taking in this case $\lim S = 7.4$ counts, while the detection efficiency is 3.9%, one can obtain the following half-life limit on the $0\nu KL$ process in ^{84}Sr :

$$T_{1/2}^{0\nu KL}(\text{g.s.} \rightarrow \text{g.s.}) \geq 1.9 \times 10^{16} \text{ yr}.$$

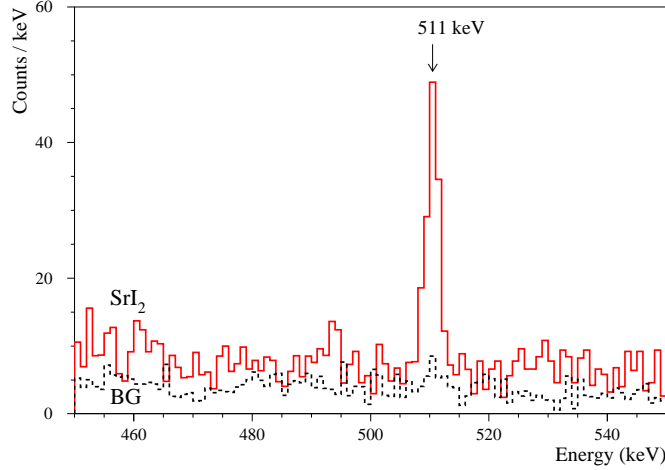


Figure 11: (Color online) Energy spectra accumulated with the $\text{SrI}_2(\text{Eu})$ sample over 706 h, and without sample over 1046 h (BG) by ultra-low background HPGe γ spectrometer deep underground. The spectra are normalized on the time of the measurements with the $\text{SrI}_2(\text{Eu})$ sample.

To search for the double electron capture of ^{84}Sr to the excited level 2^+ of ^{84}Kr , the experimental data were fitted in the energy interval (868 – 896) keV by a Gaussian function (to describe the gamma peak with the energy of 881.6 keV) and a polynomial function of second degree (to approximate the background, see Fig. 12, b). The fit gives an area of $S = (-1.2 \pm 4.9)$ counts for the double β process searched for, giving no evidence for the effect ($\text{lim } S = 6.9$ counts). Taking into account the detection efficiency for γ quanta with energy 882 keV (5.8%), we set the following limit on the process:

$$T_{1/2}^{2\nu 2\varepsilon}(\text{g.s.} \rightarrow 881.6 \text{ keV}) \geq 3.1 \times 10^{16} \text{ yr.}$$

In the neutrinoless 2ε capture to the 2^+ level, two γ quanta should be emitted. The interaction of the additional $\simeq 0.9$ MeV γ quantum with the HPGe detector slightly decreases the efficiency for the 882 keV peak (5.0%) leading to the limit:

$$T_{1/2}^{0\nu 2\varepsilon}(\text{g.s.} \rightarrow 881.6 \text{ keV}) \geq 2.6 \times 10^{16} \text{ yr.}$$

All the half-life limits on 2β decay processes in ^{84}Sr , obtained in the present experiment, are summarized in Table 4. Previously, only one limit

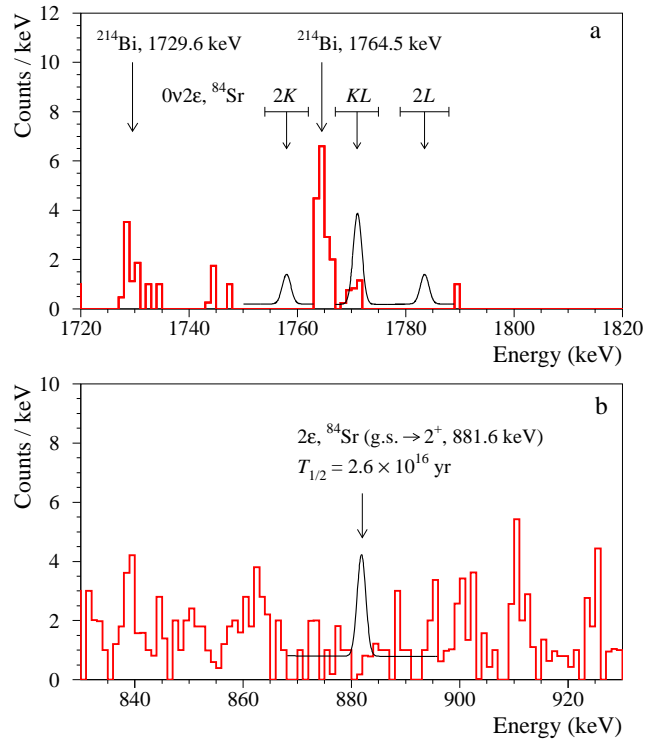


Figure 12: (Color online) (a) Part of the energy spectrum measured with the $\text{SrI}_2(\text{Eu})$ sample in the energy region where peaks from the $0\nu 2\varepsilon$ processes in ^{84}Sr ($2K$, KL and $2L$) to the ground state of ^{84}Kr are expected. The excluded peaks for the processes are shown by solid lines. (b) Part of the spectrum in the energy interval (830 – 930) keV where a γ peak with the energy of 881.6 keV is expected for the 2ε decay of ^{84}Sr to the excited level 2^+ of ^{84}Kr . The area of the peak, shown by solid line, corresponds to the half-life 2.6×10^{16} yr excluded at 90% C.L.

on $0\nu\varepsilon\beta^+$ mode was known; it was derived in [35] on the basis of the data of an old experiment with photoemulsions [36], and is two orders of magnitude lower than the one obtained in this work. It should be also noted that an experiment to search for 2β decays in ^{84}Sr with SrCl_2 crystal scintillator ($\varnothing 2 \times 1.5$ cm) with 4π CsI(Tl) active shielding is in progress in the Yang-Yang underground laboratory [37] which has a potential to improve the limits presented here.

Table 4: Half-life limits on 2β processes in ^{84}Sr . The energies of the γ lines (E_γ), which were used to set the $T_{1/2}$ limits, are listed in column 4 with the corresponding detection efficiencies (η) in column 5. The $T_{1/2}$ limits are derived in the present work at 90% C.L., while the limit from [35, 36] is given at 68% C.L.

Process of decay	Decay mode	Level of daughter nucleus (keV)	E_γ (keV)	η	$T_{1/2}$ (yr)	
					Present work	[35, 36]
$\varepsilon\beta^+$	0ν	g.s.	511	7.2%	$> 6.9 \times 10^{15}$	$> 7.3 \times 10^{13}$
$\varepsilon\beta^+$	2ν	g.s.	511	7.2%	$> 6.9 \times 10^{15}$	–
$2K$	0ν	g.s.	1754 – 1762	4.0%	$> 6.0 \times 10^{16}$	–
KL	0ν	g.s.	1767 – 1775	3.9%	$> 1.9 \times 10^{16}$	–
$2L$	0ν	g.s.	1779 – 1788	3.9%	$> 5.9 \times 10^{16}$	–
2ε	0ν	2^+ 881.6	881.6	5.0%	$> 2.6 \times 10^{16}$	–
2ε	2ν	2^+ 881.6	881.6	5.8%	$> 3.1 \times 10^{16}$	–

4. Conclusions

The radioactive contamination of the $\text{SrI}_2(\text{Eu})$ crystal scintillator obtained using a Stockbarger growth technique was estimated with the help of two approaches: by low background measurements in scintillation mode at sea level, and with the help of ultra-low background HPGe γ ray spectrometry deep underground. We have found a contamination of the scintillator by ^{137}Cs , ^{226}Ra and ^{228}Th on the level of 0.05 Bq/kg, 0.1 Bq/kg and 0.01 Bq/kg, respectively. Only limits were set on the contamination of the detector by ^{138}La at level of ≤ 0.02 Bq/kg, while the activities of ^{40}K , ^{90}Sr , ^{152}Eu ,

^{154}Eu , ^{176}Lu are below the detection limits of (0.1 – 0.3) Bq/kg. The intrinsic radiopurity of the $\text{SrI}_2(\text{Eu})$ scintillator is still far from $\text{NaI}(\text{Tl})$ and $\text{CsI}(\text{Tl})$ scintillators developed for low counting experiments, while it is three orders of magnitude better than that of the scintillation materials containing La, and five orders of magnitude better than that of the scintillators containing Lu.

The response of the $\text{SrI}_2(\text{Eu})$ crystal scintillator to α particles was estimated by using the trace contamination of the crystal by ^{226}Ra . The α/β ratio was measured as 0.55 for 7.7 MeV α particles of ^{214}Po . No difference in pulse shapes of scintillation for γ quanta and α particles was observed (the decay time was estimated to be: $\approx 1.7 \mu\text{s}$).

Applicability of $\text{SrI}_2(\text{Eu})$ crystal scintillators to the search for the double beta decay of ^{84}Sr was demonstrated for the first time. New improved half-life limits were set on double electron capture and electron capture with positron emission in ^{84}Sr at level of $T_{1/2} \sim 10^{15} - 10^{16}$ yr.

The results of these studies demonstrate the possible perspective of the $\text{SrI}_2(\text{Eu})$ highly efficient scintillation material in a variety of applications, including low counting measurements.

An R&D of $\text{SrI}_2(\text{Eu})$ crystal scintillators is in progress. We are going to study radioactive contaminations of larger volume $\text{SrI}_2(\text{Eu})$ crystal scintillators both by ultra-low background HPGe γ spectrometry and low background scintillation counting at the Gran Sasso National Laboratory.

5. Acknowledgments

The work of the INR Kyiv group was supported in part by the Project “Kosmomikrofizyka-2” (Astroparticle Physics) of the National Academy of Sciences of Ukraine.

References

- [1] R. Hofstadter, U.S. Patent No. 3,373,279 (March 12, 1968).
- [2] N.J. Cherepy et al., Appl. Phys. Lett. 92 (2008) 083508.
- [3] N.J. Cherepy et al., IEEE Trans. Nucl. Sci. 56 (2009) 873.
- [4] E.V. van Loef et al., IEEE Trans. Nucl. Sci. 56 (2009) 869.
- [5] M.S. Alekhin et al., IEEE Trans. Nucl. Sci. 58 (2011) 2519.

- [6] H. Tan, W.K. Warburton, Nucl. Instr. Meth. A 652 (2011) 221.
- [7] J. Glodo et al., IEEE Trans. Nucl. Sci. 57 (2010) 1228.
- [8] B.W. Sturm et al., Nucl. Instr. Meth. A 652 (2011) 242.
- [9] N.J. Cherepy et al., "SrI₂ scintillator for gamma ray spectroscopy", Proceedings of SPIE – The International Society for Optical Engineering, vol. 7449 (2009) art. no. 74490F.
- [10] D. C. Stockbarger, Rev. Sci. Instrum. 7 (1936) 133.
- [11] P. Dorenbos, J.T.M. de Haas, C.W.E. van Eijk, IEEE Trans. Nucl. Sci. 42 (1995) 2190.
- [12] M. Moszyński, Nucl. Instr. Meth. A 505 (2003) 101.
- [13] T. Fazzini et al., Nucl. Instr. Meth. A 410 (1998) 213.
- [14] F.A. Danevich et al., Phys. Rev. C 67 (2003) 014310.
- [15] P. Belli et al., Phys. Rev. C 76 (2007) 064603.
- [16] R.B. Firestone et al., *Table of Isotopes*, 8-th ed., John Wiley, New York, 1996 and CD update, 1998.
- [17] E.V. Sysoeva et al., Nucl. Instr. Meth. A 414 (1998) 274.
- [18] R. Bernabei et al., Nucl. Instr. Meth. A 592 (2008) 297.
- [19] P. Belli et al., Nucl. Phys. A 826 (2009) 256.
- [20] F.A. Danevich et al., Phys. Lett. B 344 (1995) 72.
- [21] F.A. Danevich et al., Nucl. Phys. A 694 (2001) 375.
- [22] J.H. Reeves et al., IEEE Trans. Nucl. Sci. NS-31 (1984) 697.
- [23] N. Kamikubota et al., Nucl. Instr. Meth. A 245 (1986) 379.
- [24] C. Arpesella, Appl. Radiat. Isot. 47 (1996) 991.
- [25] T. Iwawaki et al., Natural Science Research 11 (1998) 1.

- [26] S. Agostinelli et al., Nucl. Instr. Meth. A 506 (2003) 250;
J. Allison et al., IEEE Trans. Nucl. Sci. 53 (2006) 270.
- [27] O.A. Ponkratenko et al., Phys. At. Nucl. 63 (2000) 1282;
V.I. Tretyak, to be published.
- [28] C. Arpesella et al., Astropart. Phys. 18 (2002) 1.
- [29] M. Laubenstein et al., Appl. Radiat. Isot. 61 (2004) 167.
- [30] H.S. Lee et al., Nucl. Instr. Meth. A 571 (2007) 644.
- [31] M. Berglund and M.E. Wieser, Pure Appl. Chem. 83 (2011) 397.
- [32] R. Bernabei et al., Nucl. Instr. Meth. A 555 (2005) 270.
- [33] G. Audi, A.H. Wapstra, C. Thibault, Nucl. Phys. A 337 (2003) 729.
- [34] G.J. Feldman, R.D. Cousins, Phys. Rev. D 57 (1998) 3873.
- [35] V.I. Tretyak, Yu.G. Zdesenko, At. Data Nucl. Data Tables 61 (1995) 43;
80 (2002) 83.
- [36] J.H. Fremlin, M.C. Walters, Proc. Phys. Soc. A 65 (1952) 911.
- [37] G. Rooh et al., IEEE Trans. Nucl. Sci. 55 (2008) 1445.